arXiv:2601.23251v2 [cs.CV] 8 May 2026

Structure Over Scale: Learning Visual Reasoning from Pedagogical Video

Bishoy Galoaa*
Northeastern University
galoaa.b@northeastern.edu

Xiangyu Bai*
Northeastern University
bai.xiang@northeastern.edu

Sarah Ostadabbas
Northeastern University
s.ostadabbas@northeastern.edu

Abstract

State-of-the-art vision-language models (VLMs) score impressively on video benchmarks yet stumble on basic visual reasoning tasks involving spatial relations, navigation, and object selection that a preschooler solves easily. We hypothesize that the explicit pedagogical structure, specifically the *context-question-pause-answer* cycles embedded in children's educational video, provides naturally co-aligned reasoning traces: temporally synchronized visual cues, questions, and answers that emerge only from deliberate pedagogical authoring and cannot be practically reconstructed through manual annotation at scale. To test this, we introduce **SoSVQA** (Structure over Scale Visual Question Answering), a unified benchmark of 10K question-answer pairs automatically extracted from *Dora the Explorer* (DoraVQA) and *Mickey Mouse Clubhouse* (ClubHVQA) with precise timestamp alignment, and fine-tune Qwen2-VL and Qwen3-VL using Group Relative Policy Optimization (GRPO) to leverage the clear correctness signals and structured reasoning traces inherent in educational content. Despite training on just 10K QA pairs from 78 hours of children's television, orders of magnitude less data than GPT and Gemini, our approach delivers generalizable performance gains for Qwen-based VLMs, yielding consistent improvements on NExT-QA (+19.7), Video-MME (+10.6), and MotionBench (+4.9), matching the performance of leading proprietary systems and demonstrating that content structure can compensate for content scale. Code is available at ostadabbas/SoS.

1 Introduction

Despite achieving strong performance [33, 32], today's vision-language models fail systematically at the simple reasoning tasks that children master before kindergarten. On diagnostic benchmarks targeting objects, spatial relations, and directional understanding, state-of-the-art models such as GPT-5.5 and Gemini 3.1 Pro achieve only 60–70% accuracy [23, 6], far below the 95%+ performance observed in humans [8]. These failures persist even in simple scenes [26], suggesting that gains in video understanding often arise from scaling data volume and statistical pattern matching rather than grounded reasoning. Modern data-centric models largely memorize surface level patterns: state-of-the-art VLMs display only superficial reasoning, mirroring patterns from large-scale, generic video-text pairs rather than genuinely learning spatial relational reasoning. We argue that effective learning of spatial concepts requires not only large data corpus, but also repeated, explicit supervision that grounds language to visual evidence through instruction, feedback, and temporal scaffolding.

Preprint.

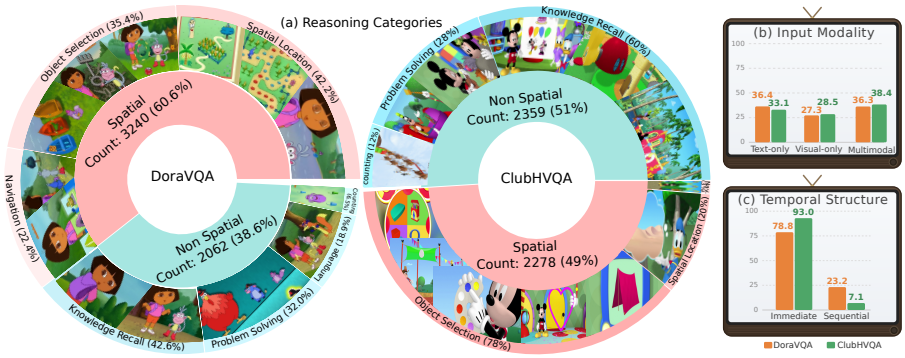


Figure 1: **SoSVQA** (Structure over Scale Visual Question Answering) dataset composition across two subsets: DoraVQA and ClubHVQA. **(a) Reasoning categories:** DoraVQA is dominated by spatial-reasoning tasks, whereas ClubHVQA emphasizes object-selection and knowledge-recall tasks. **(b) Input modality:** Both datasets exhibit similar input modality distributions. **(c) Temporal structure:** ClubHVQA predominantly requires immediate reasoning, whereas DoraVQA includes a substantially larger portion of sequential-reasoning questions.

Children's educational television offers this uniquely structured alternative. Programs such as *Dora the Explorer* [27] and *Mickey Mouse Clubhouse* [9] are explicitly designed around a consistent *context-question-pause-answer* pedagogical loop: each episode establishes visual context, poses direct spatial questions to the viewer, and then pauses (visually "hinting" at the answer by overlaying directional arrows, zooms, and character gestures that isolate the exact evidence needed to answer) before revealing an unambiguous answer with verbal explanation. This pause segment functions as an implicit reasoning trace, encoding two distinct learning signals that we later isolate experimentally (Section B): a spatial attention signal (where to look, recoverable through the visual hints) and an entity grounding signal (what it is called). The structure recurs systematically across every entry, generating 15–20 explicit question-answer pairs with clear correctness signals per episode.

This pedagogical design produces measurable learning gains in children [16, 2, 3], with controlled studies showing that preschoolers who watch *Dora the Explorer* score significantly higher on direction/position concepts and spatial ability tasks than children who do not [3], confirming that the pause structure carries genuine supervisory signal. We hypothesize that the same structure that supports human learning can serve as an efficient and underexplored training signal for vision language models. This observation points to a broader scalable data strategy: rather than blindly rely on increasing data scale; we need data that knows how to *teach*. Fortunately, the world contains a large supply of pedagogically structured content that has never been used this way: children's television, Khan Academy lectures, PhET simulations, and similar resources all embed explicit teaching signals in their design. To test this hypothesis, we introduce **SoSVQA** (Structure over Scale Visual Question Answering), a unified benchmark of 10K question-answer pairs, containing two sub-datasets extracted from children's educational television: **DoraVQA**, comprising 5,348 question-answer pairs from 8 seasons (96 episodes) of *Dora the Explorer*, and **ClubHVQA** (ClubhouseVQA), comprising 4,652 question-answer pairs from 4 seasons (132 episodes) of *Mickey Mouse Clubhouse*. Each example preserves the show's pedagogical structure (context, question, pause, and answer) with corresponding video timestamps and pause-based visual context extracted via an LLM agent.

To test whether structured supervision transfers beyond its source content, we fine-tune Qwen2-VL [28] and Qwen3-VL [4] using Group Relative Policy Optimization (GRPO) [21], which naturally aligns with educational content: answers are objectively correct or incorrect, and the show's explanations provide implicit reasoning cues without manual annotation. Rather than adapting models to specific content, our goal is to improve spatial reasoning abilities using structured learning format already embedded in the data. We evaluate along three axes: (i) **in-domain** performance on DoraVQA and ClubHVQA, (ii) **cross-show** transfer between the two subsets to test whether learning generalizes across pedagogical content rather than memorizing show-specific patterns, and (iii) **cross-benchmark** transfer to Video-MME [7], NExT-QA [32], MVBench [14], MotionBench [11], and TVBench [5]. We train on open-ended answer generation but evaluate on multiple-choice benchmarks throughout, a deliberate format mismatch that distinguishes transferable reasoning from answer-format memorization. We additionally probe whether the show's *pause hints* are recoverable by prompting alone or require structured supervision (Section B), separating spatial attention from entity grounding as distinct learning signals.

Our contribution can be listed as follows:

- We show that the *context-question-pause-answer* structure of children's educational television serves as implicit reasoning supervision for VLMs, yielding cross-benchmark spatial reasoning improvements without large-scale data.
- We present an automated pipeline that extracts self-supervised training data from pedagogically structured video, preserving the correctness signals embedded in its reasoning structure without manual annotation. We validate the pipeline across two shows with distinct reasoning profiles, and additionally release manually annotated bounding-box hints for the pause-segment visual cues to support future spatial-grounding work.
- We introduce **SoSVQA**, a benchmark of 10K question-answer pairs automatically extracted from *Dora the Explorer* and *Mickey Mouse Clubhouse* with precise timestamp alignment. SoSVQA is the first video question-answering datasets extracted from children's educational television, with temporal alignment between visual frames, questions, context, and answers.

2 Related Work

VLMs and Video Understanding. Recent work has scaled VLMs to capture temporal dynamics beyond images. Video-LLaVA [15] demonstrated that joint training on videos and images improves both modalities through unified visual representations; InternVideo2 [30] expanded video encoders using progressive training and masked video modeling; LLaVA-Video [35] introduced dense frame sampling to capture fine-grained temporal dynamics. However, these approaches train predominantly on web videos [17, 1, 12], which contain diverse content but lack explicit pedagogical structure. While these videos display spatial relationships and temporal sequences, they rarely verbalize spatial concepts explicitly or provide structured question-answer pairs that ground visual patterns in linguistic descriptions. Our work differs by leveraging educational content where spatial reasoning is explicitly taught through scaffolded question-answer sequences with clear correctness signals.

Spatial Reasoning in VLMs. Despite achieving strong performance on existing video benchmarks [32, 33], VLMs exhibit systematic failures on spatial reasoning tasks. Fu et al. [8] reveals that VLMs achieve only half of human accuracy with noticeable failures on spatial reasoning tasks. Tong et al. [26] demonstrated that current VLMs are barely above random chance on tasks requiring precise spatial understanding. These failures extend to fundamental spatial primitives: models struggle with counting objects beyond small numbers [18], fail at compositional spatial relationships [25], and fail to reason about object positions across video frames [20]. Importantly, these deficiencies persist even in simple visual scenes with minimal occlusion and clear object boundaries, indicating that the limitation is not perceptual but conceptual: models lack the structured spatial reasoning that children acquire through explicit instruction.

Educational and Instructional Video as Training Data. Instructional videos have been explored as training data for procedure understanding and action recognition. Miech et al. [17] demonstrated that instructional videos provide natural language supervision for video-text embeddings. However, the narrations describe actions chain rather than teaching concepts; The CrossTask [36] and COIN [24] datasets extract procedural steps from instructional videos but focus on temporal ordering rather than spatial reasoning. Although these datasets compose of structured contents, they are not explicit question-answer structure that "teaches" spatial reasoning. Closest to our work, Anderson and Burns [2] analyzed the pedagogical structure of children's educational television, documenting how the question-pause-answer format creates structured learning opportunities. We build on this insight by extracting the explicit question-pause-answer pairs from educational content as direct supervision signals, leveraging the pedagogical design for model training rather than treating video as passive observation. Adjacent work has trained VLMs on infant egocentric video [29], but no prior work has used the pedagogical structure of children's television as a direct training signal for VLMs.

Reinforcement Learning for VLM Fine-tuning. Group Relative Policy Optimization (GRPO) [21] has emerged as an efficient alternative to Proximal policy optimization (PPO) [19] for reasoning tasks: DeepSeek-R1 [10] demonstrated that GRPO with rule-based rewards achieves reasoning capabilities competitive with proprietary models. Recent work has successfully applied GRPO to vision-language tasks: VLM-R1 [22] showed that GRPO fine-tuning achieves superior out-of-distribution generalization compared to SFT on visual reasoning tasks, while CrowdVLM-R1 [31] developed specialized reward functions for counting tasks in crowded scenes. These works primarily

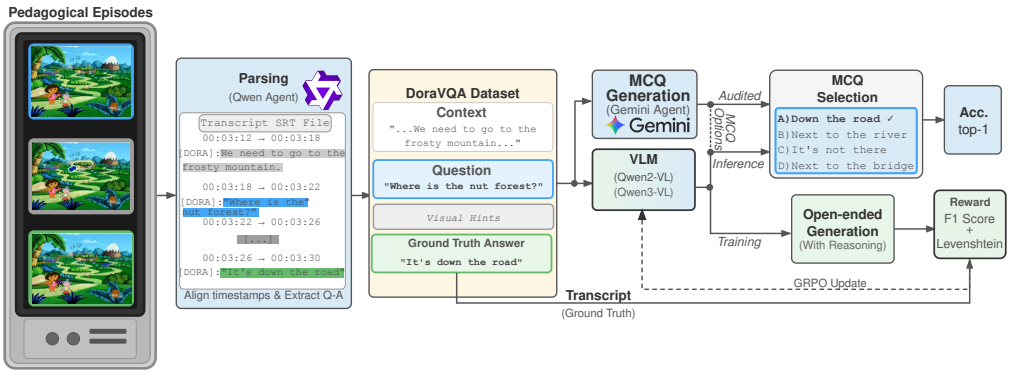


Figure 2: **SoSVQA pipeline overview.** We extract question-answer pairs from pedagogical episodes by parsing SubRip Text (SRT) transcript files with a Qwen agent, aligning timestamps to identify the show's pedagogical *context-question-pause-answer* structure. Each question is paired with its surrounding context window, the ground truth answer, and multiple-choice distractors (MCQs) that follows. During training, we fine-tune Qwen models using GRPO on open-ended generation; during inference, the MCQ options are provided to our fine-tuned models, creating a deliberate train-test format mismatch (open-ended $\rightarrow$ MCQ) that evaluates transferable reasoning.

design reward models for general-purpose instruction following. In contrast, we apply GRPO to pedagogically-structured video content where the reward signal is implicit in the educational design, where ground-truth answers are directly in its structure. This eliminates the need for external reward model while providing clear correctness signals, creating a self-supervised RL training environment where the pedagogical content naturally defines the learning objectives.

Our work is positioned at the intersection of these research directions: we address video-language model spatial reasoning failures by training on content that explicitly teaches spatial concepts through structured question-answer pairs. Unlike general instructional videos that show only procedures, educational television teaches reasoning through direct instruction, repetition, and scaffolded examples. We leverage this pedagogical structure with GRPO fine-tuning, using the natural correctness signals from educational content as supervision without requiring manual annotation or reward engineering.

3 Method

3.1 SoSVQA: Structure and Formatting

We operationalize the *context-question-pause-answer* structure of educational television as a multimodal training example (Figure 2). Each example in the SoSVQA dataset $\mathcal{D}$ is formatted as $x = \{I, T, Q, a^*\} \in \mathcal{D}$, where I represents the visual frames sampled before and at the question timestamp, T is the transcript providing narrative context within a fixed time window before the question, Q is the explicit question and a^* is ground truth answer. We treat I and T as separate input streams rather than collapsing them, allowing the model to draw on visual scene evidence and linguistic context independently before fusion. The ground-truth answer a^* is always either directly stated in the transcript or deducible in a single inferential step, providing an unambiguous reward target without manual annotation. The model receives x as a structured multimodal prompt (visual frames embedded alongside a text sequence concatenating the system instruction, transcript context, and question) and generates a distribution over answer tokens that is trained toward a^* via the reward signal described in Section 3.2.

3.2 Group Relative Policy Optimization (GRPO)

We fine-tune using GRPO [21], which optimizes a policy π_θ without a separate value network by computing advantages relative to a group of sampled outputs. GRPO is well-suited here because educational content provides objectively correct answers, eliminating the need for complex reward modeling. For each input $x \in \mathcal{D}$, the policy samples K candidate answers $\{a_1, \ldots, a_K\}$. Each candidate is scored against the ground-truth a^* via:

$$r(a_i, a^*) = \alpha \, \mathrm{F1}(a_i, a^*) + \beta \left(1 - \frac{\mathrm{lev}(a_i, a^*)}{\max(|a_i|, |a^*|)}\right), \tag{1}$$

Algorithm 1 GRPO Training with Context-Question-Pause-Answer Structure

Require: Dataset $\mathcal{D}$ of x=$\{I, T, Q, a^*\}$; policy π_θ; reference π_{ref}; group size K; weights α, β, λ; learning rate η

for each mini-batch $\mathcal{B} \sim \mathcal{D}$ **do**
  for all $x \in \mathcal{B}$ **do**
    Sample $\{a_i\}_{i=1}^{K} \sim \pi_\theta(\cdot \mid I, T, Q)$
    $r_i \leftarrow \alpha\,\text{F1}(a_i, a^*) + \beta\Big(1 - \frac{\text{lev}(a_i, a^*)}{\max(|a_i|, |a^*|)}\Big)$
    $A_i \leftarrow r_i - \frac{1}{K}\sum_j r_j$
  end for
  $\theta \leftarrow \theta - \eta\,\nabla_\theta \sum_{x,i}[-A_i \log \pi_\theta(a_i \mid x) + \lambda\, D_{\text{KL}}(\pi_\theta \,\|\, \pi_{\text{ref}})]$
end for

where $\text{F1}(a_i, a^*)$ measures token-level semantic overlap, $\text{lev}(a_i, a^*)$ is the Levenshtein edit distance normalized by the length of the longer string $\max(|a_i|, |a^*|)$, and $\alpha = 0.3$, $\beta = 0.7$ are fixed weights selected by empirical validation (see Appendix A), with $\alpha+\beta = 1$. The two terms are complementary: F1 tolerates minor surface variation while normalized Levenshtein penalizes character-level errors and near-miss re-orderings. This yields a stable continuous signal; exact matches score 1.0, semantically correct answers with minor variation score 0.65–0.95, and incorrect answers score near zero.

For a group of K sampled candidates with rewards $\{r(a_1, a^*), \ldots, r(a_K, a^*)\}$, the advantage for candidate a_i is computed relative to the group mean:

$$A(a_i, a^*) = r(a_i, a^*) - \frac{1}{K}\sum_{j=1}^{K} r(a_j, a^*), \tag{2}$$

so that the policy is updated toward outputs that outperform the group average rather than toward an absolute value target. The training objective is:

$$\mathcal{L}(\theta) = -\mathbb{E}_{x\sim\mathcal{D},\, a_i\sim\pi_\theta(\cdot|x)}\left[A(a_i, a^*) \log \pi_\theta(a_i|x)\right]. \tag{3}$$

Critically, the reward in Eq. 1 is computed against free-form a^* during training, while evaluation uses multiple-choice prompting. This deliberate format mismatch tests whether gains reflect transferable reasoning rather than answer-format memorization.

3.3 GRPO Training

The GRPO training procedure for the *context-question-pause-answer* structure is presented in Algorithm 1 and illustrated in Figure 2. For each multimodal input $x \in \mathcal{D}$, the policy π_θ generates K candidate answers $\{a_1, \ldots, a_K\}$ via temperature sampling (temperature $= 1.0$, top-$p = 0.9$). Each candidate a_i is evaluated against the ground-truth answer a^* using the reward function $r(a_i, a^*)$ defined in Section 3.2, and group-relative advantages $A(a_i, a^*)$ are computed over the K generations. The policy parameters θ are updated by minimizing $\mathcal{L}(\theta)$ to maximize the expected group-relative advantage. To stabilize training, a KL divergence penalty is added between the updated policy π_θ and a frozen reference policy π_{ref}:

$$\mathcal{L}_{\text{KL}}(\theta) = \mathcal{L}(\theta) + \lambda\,\mathbb{E}_{x\sim\mathcal{D}}\left[D_{\text{KL}}(\pi_\theta(\cdot|x) \,\|\, \pi_{\text{ref}}(\cdot|x))\right], \tag{4}$$

where $\lambda = 0.01$ is the KL coefficient. Unless otherwise noted, models are trained jointly on both SoSVQA splits; single-show training is used only in the cross-show ablation (Table 4). Training hyperparameters (learning rate $\eta = 1 \times 10^{-4}$, reward scaling factor $s = 2.0$, and group size $K = 8$) are selected via sequential sweeps on held-out validation data (Appendix A).

4 Experiments and Results

We evaluate our approach along three axes designed to test the structure-over-scale hypothesis. First, *in-domain* performance on both SoSVQA splits (DoraVQA and ClubHVQA) tests whether the *context-question-pause-answer* structure was learned at all, and contamination analysis verifies that improvements come from visual grounding rather than pre-training memorization. Second,

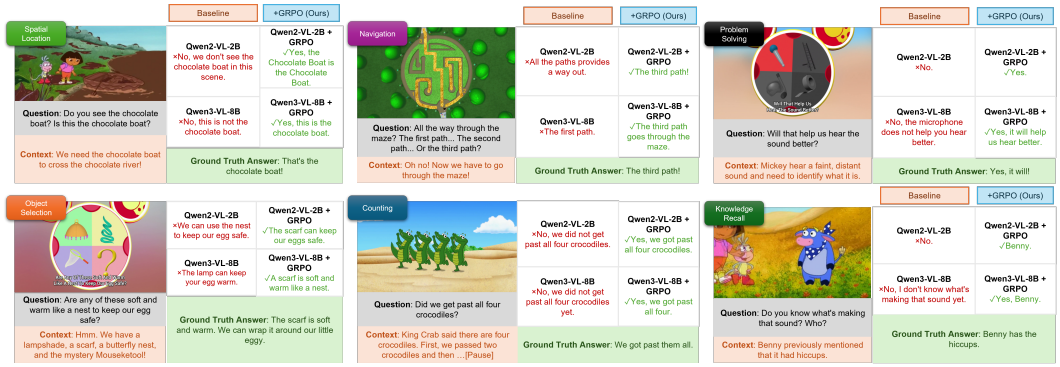


Figure 3: **Qualitative comparison on some samples of challenging spatial reasoning tasks.** Our GRPO-finetuned models (blue) outperform all baselines (orange) across every reasoning category. While baseline models frequently fail or hallucinate, our models consistently produce accurate and concise answers. See Appendix C and supplementary material for more examples.

Table 1: Performance comparison on DoraVQA and ClubHVQA test sets across reasoning categories. Our **+ GRPO** models are fine-tuned jointly on the union of DoraVQA and ClubHVQA training splits. Gray rows indicate proprietary models; underlined scores indicate results surpassed by our best model (Qwen3-VL-8B + GRPO). Green indicates improvement over baseline, red indicates degradation. All results are reported using top-1 accuracy.

	Overall		Spatial		Obj. Selection & Counting		Navigation		Knowledge	
Model										
Gemini-3.0-Flash	76.10	69.16	67.83	62.18	87.10	73.10	65.38	65.91	88.52	68.57
Gemini-3.0-Flash (low thinking)	75.84	63.96	66.81	54.98	88.17	68.52	69.23	61.36	86.89	60.83
GPT-4V	67.79	68.20	60.34	64.10	75.27	69.90	69.23	65.91	68.85	66.15
Gemini-2.5-Pro	64.41	62.69	62.62	52.92	72.83	70.53	60.78	65.91	71.93	60.00
LLaVA-Video-7B	55.41	46.46	54.02	45.10	62.22	54.52	66.00	47.62	67.31	48.66
Video-LLaVA-7B	37.82	39.19	47.49	41.48	60.66	42.78	46.34	56.76	32.43	40.68
InternVideo2.5-8B	57.68	50.10	46.55	49.52	63.04	55.87	59.62	36.36	68.85	53.14
Qwen2-VL-2B (baseline)	40.29	31.43	45.36	33.99	37.61	36.10	39.03	23.26	39.95	32.87
Qwen2-VL-2B + GRPO	**48.32** (+8.03)	**36.68** (+5.25)	**58.86** (+13.50)	**45.21** (+11.22)	**44.71** (+7.10)	**42.38** (+6.28)	**44.30** (+5.27)	**46.51** (+23.25)	**45.97** (+6.02)	**38.07** (+5.20)
Qwen2-VL-7B (baseline)	52.21	45.09	54.14	44.55	51.45	49.51	41.97	40.91	48.77	48.05
Qwen2-VL-7B + GRPO	**57.68** (+5.47)	**50.10** (+5.01)	**67.25** (+13.11)	**50.97** (+6.42)	**64.37** (+12.92)	**58.98** (+9.47)	**47.80** (+5.83)	**50.00** (+9.09)	**67.25** (+18.48)	**54.49** (+6.44)
Qwen3-VL-8B (baseline)	55.24	50.67	57.17	49.20	53.58	58.62	**48.96**	45.45	50.32	50.50
Qwen3-VL-8B + GRPO	**62.98** (+7.74)	**56.81** (+1.57)	**69.65** (+12.48)	**59.16** (+1.99)	**64.59** (+11.01)	**64.87** (+6.25)	48.33 (-0.63)	**60.74** (+15.29)	**55.12** (+4.80)	**57.48** (+6.98)

cross-show transfer between DoraVQA and ClubHVQA tests whether learning generalizes across pedagogical content rather than memorizing show-specific patterns. Third, *cross-benchmark* transfer to six external video-understanding benchmarks tests whether the learning generalizes beyond children's educational content, and ablations isolate which components drive the gains.

4.1 Datasets

We evaluate on in-domain SoSVQA (DoraVQA and ClubHVQA) and a broad set of out-of-domain external benchmarks selected to test the transferability of spatial reasoning improvements. Our models achieve strong gains across all benchmarks, ruling out narrow overfitting to a single evaluation style.

SoSVQA. The two SoSVQA subsets contain a combined total of 10,000 QA pairs and follow a consistent *context–question–pause–answer* pedagogical structure with clear ground-truth supervision, but exhibit complementary reasoning profiles (Figure 1): DoraVQA (5,348 pairs) is spatial-heavy (60.6%) with strong navigation demands, while ClubHVQA (4,652 pairs) is balanced between spatial and non-spatial tasks (49%/51%) and dominated by object selection (78%). We do not redistribute video frames or audio; we release only episode identifiers, timestamps, QA annotations, the annotation pipeline, and manually annotated bounding-boxes for the pause-segment visual cues. Multiple-choice options are generated from the free-form gold answers via Gemini 2.5 Flash and manually audited to prevent surface-form shortcuts (Appendix F).

Video-MME [7] evaluates multimodal LLMs across short, medium, and long videos using visual, subtitle, and audio cues; we report the short partition. **NExT-QA** [32] tests causal and temporal reasoning through "why" and "how" questions. **MVBench** [14] covers 20 temporal video-understanding tasks designed to require multi-frame reasoning. **MotionBench** [11] evaluates fine-grained motion comprehension through six motion-oriented question categories. **TVBench** [5] isolates temporal reasoning by removing the spatial, textual, and world-knowledge shortcuts present in earlier benchmarks.

Table 2: Cross-benchmark transfer evaluation highlighting **structure vs. scale**. Despite fine-tuning on only 10K QA pairs (78 hours), our models achieve competitive or state-of-the-art results against models trained on orders of magnitude more data. proprietary models; our state-of-the-art result; our minimal fine-tuning addition. Green indicates improvement over baseline. † indicates zero-shot evaluation; * indicates training set seen during pre-training. Our GRPO models share the same pre-training corpus as their baselines but additionally fine-tune jointly on the 10K pedagogically-structured QA pairs from SoSVQA (78 hours of educational video).

Model	Params	Scale	V-MME	NExT-QA	MVBench	MotionBench	TVBench
GPT-4V†	∼1.8T	∼10T tokens	59.9	68.2	43.50	58.82	34.00
Gemini-2.5-Pro†	–	–	85.2	74.6	45.50	66.30	46.50
Gemini-3.0-Flash†	–	–	**86.9**	80.4	65.50	70.40	38.25
InternVideo2.5-8B	8B	16M clips	65.4	71.5*	75.7	45.56	48.80
LLaVA-Video-7B	7B	1.3M videos	63.3	**83.2***	69.7	48.29	42.30
Video-LLaVA-7B	7B	760K videos	45.3	52.1*	40.95	35.72	36.30
Qwen2-VL-2B (baseline)	2B	1.2T tokens	50.10	52.60	58.99	47.0	39.85
Qwen2-VL-2B + GRPO†	2B	1.2T + **10K QA**	**60.74** (+10.64)	**72.11** (+19.51)	**59.94** (+0.95)	51.92 (+4.92)	40.05 (+0.80)
Qwen2-VL-7B (baseline)	7B	1.2T tokens	67.50	67.0	**65.49**	52.0	**40.75**
Qwen2-VL-7B + GRPO†	7B	1.2T + **10K QA**	**69.25** (+1.75)	**81.80** (+12.46)	64.33 (-1.16)	**54.01** (+2.01)	40.60 (-0.15)
Qwen3-VL-8B (baseline)	8B	1.0T tokens	71.40	62.1	**68.70**	**61.12**	46.53
Qwen3-VL-8B + GRPO†	8B	1.0T + **10K QA**	**80.00** (+8.60)	**81.80**† (+19.70)	67.59 (-1.11)	61.03 (-0.09)	47.48 (+0.95)

4.2 In-Domain Performance on SoSVQA

Table 1 reports per-category performance on both DoraVQA and ClubHVQA, testing whether the *context-question-pause-answer* structure was learned. GRPO fine-tuning produces large, structurally-aligned gains on the two categories most directly targeted by the show's pedagogical pause: spatial reasoning improves by +11 to +13 points across all DoraVQA rows, and navigation gains as much as +23.25 (Qwen2-VL-2B) and +15.29 (Qwen3-VL-8B) on ClubHVQA, reflecting the dataset's visually-driven structure. Object selection and counting improve consistently across subsets (+6 to +13 points), and knowledge recall transfers strongly, peaking at +18.48 for Qwen2-VL-7B on DoraVQA. These per-category gains aggregate into consistent overall improvements of +5.47 to +8.03 on DoraVQA and +1.57 to +5.25 on ClubHVQA, with larger relative gains on smaller models. The lone regression is Qwen3-VL-8B's navigation on DoraVQA (-0.63), where the baseline already operates near saturation. Figure 3 shows representative qualitative improvements.

4.3 Cross-Benchmark Transfer

Table 2 provides empirical support for our structure-over-scale hypothesis: structured pedagogical training induces reasoning capabilities that generalize beyond the narrow domain of children's educational content. With only 10K QA pairs (78 hours), our GRPO-finetuned models match or exceed proprietary systems trained on orders of magnitude more data on multiple external benchmarks. Crucially, all external evaluation uses multiple-choice prompting while training was open-ended, ruling out answer-format memorization as the source of these gains.

The largest improvements appear on **NExT-QA** [32], where all three GRPO-finetuned backbones gain +12.46 to +19.70 points, followed by **Video-MME** (+1.75 to +10.64). Both benchmarks focus on causal and temporal why/how questions that require integrating evidence across temporally separated frames. Our structured context-question-pause-answer paradigm is designed to address these problems: the question anchors to earlier context, the pause supplies the relevant visual evidence, and the answer follows. On **MVBench**, **MotionBench**, and **TVBench**, gains are small or absent, because these benchmarks emphasize fine-grained motion and bias-controlled temporal cues that the pedagogical pause does not directly target. The pattern is consistent: where the benchmark probes a reasoning skill structurally aligned with SoSVQA's pedagogical loop, transfer is large; where it does not, gains shrink. This both supports the structure-over-scale claim and delineates its scope.

4.4 Contamination Analysis

A natural concern is that gains on SoSVQA reflect textual memorization of existing TV program contents from pre-training sources, rather than genuine visual grounding. We probe each LLM backbone directly (vision encoder disabled) with factual recall and Wikipedia completion, and separately evaluate the full VLM with a blank gray image substituted for every episode frame. Table 3 shows DoraVQA is markedly more contaminated than ClubHVQA on every backbone probe. This

Table 3: Combined contamination analysis across DoraVQA and ClubHVQA. The **LLM backbone** columns (vision encoder disabled) confirm pre-training contamination via two probes: *MCQ* accuracy well above the 25% chance level on episode-specific questions, and *F1* / *Containment* on open-ended recall (Containment measures whether the gold answer appears anywhere in the model's output, regardless of phrasing). The **Full VLM** columns show this textual knowledge does not transfer to visual grounding: *Blank image* accuracy remains near chance despite the model knowing the answers textually, and the gap to *Episode frame (+ GRPO)* confirms our gains reflect structured visual learning rather than memorization.

	LLM backbone (text only)						Full VLM					
	MCQ		F1		Containment		Blank image		Episode frame (base)		Episode frame (+ GRPO)	
Model	*chance = 25%*		*chance ≈ 0%*		*chance ≈ 0%*		*chance = 25%*		*chance = 25%*		*chance = 25%*	
Qwen2-VL-2B	34.60	19.20	5.23	4.32	22.01	19.14	33.20	31.35	41.36	31.43	55.11	36.68
Qwen2-VL-7B	36.37	21.00	5.46	9.49	23.74	**23.65**	39.49	38.63	56.74	45.09	62.38	50.10
Qwen3-VL-8B	**39.23**	**27.38**	**12.07**	**11.57**	**24.64**	16.22	**44.54**	**48.87**	**58.08**	**50.45**	**67.98**	**56.81**

Table 4: Training-data ablations. **(a)** Cross-show transfer with Qwen2-VL-2B: a model trained on one SoSVQA split is evaluated on both, plus three external benchmarks. **(b)** Generic (NExT-OE) training, 10K QA, across three backbones; the gain over the SoSVQA-joint training reported in Tables 1 and 2 isolates the contribution of pedagogical structure. shaded cells denote in-domain evaluation. * indicates eval set seen during fine-tuning.

(a) Cross-show transfer (Qwen2-VL-2B)

Train	Method	In-Domain		Cross-Benchmark	
				V-MME	NExT
–	Baseline	41.36	50.35	50.10	52.60
	SFT	54.30	30.52	53.33	66.63
	GRPO	**55.11**	**54.45**	**55.40**	**72.86**
	GRPO	**67.04**	**59.92**	**77.53**	**80.25**

(b) Generic training (NExT-OE, 10K QA)

Model	In-Domain		Cross-Benchmark	
			V-MME	NExT
Qwen2-VL-2B	40.11	30.67	51.55	72.00*
Qwen2-VL-7B	53.55	44.30	65.33	82.33*
Qwen3-VL-8B	**56.20**	**50.75**	**74.44**	**83.33***

is unsurprising given Dora's verbally distinctive format ("to get to X, we go past Y") generates highly quotable text across blogs, wikis, and parenting forums, while Clubhouse is visually-driven, dominated by object selection (78%), and less represented in early web crawls. Crucially, this textual knowledge does *not* transfer to visual performance. Blank-image accuracy remains near chance for both datasets, and GRPO gains hold even on the more contaminated DoraVQA, indicating our improvements come from structured visual grounding rather than recall of pre-learned facts.

4.5 Ablation Studies

We conduct ablation studies on training strategies, input modalities, and pedagogical structure using a Qwen2-VL-2B model fine-tuned for 100 epochs on DoraVQA, evaluating performance on 10% randomly sampled test subsets of Video-MME and NExT-QA.

Training Method. Table 4 compares SFT and GRPO across the *cross-show* 2×2 matrix (DoraVQA and ClubHVQA as both train and eval) plus three external benchmarks. SFT matches GRPO in-domain (54.30 vs. 55.11 on DoraVQA) and achieves modest cross-benchmark gains, but collapses 19.83 points below baseline when evaluated on the unseen show ClubHVQA (30.52 vs. 50.35), revealing overfitting to show-specific surface patterns. GRPO generalizes in both cross-show directions, but the transfer is asymmetric: DoraVQA→ClubHVQA improves 4.10 points over baseline, while ClubHVQA→DoraVQA improves 25.68 points and even exceeds the Dora-trained GRPO on DoraVQA itself (67.04 vs. 55.11). The Mickey-trained model also produces our highest cross-benchmark scores on V-MME (77.53). This asymmetry is the cleanest test we have of the structure-versus-content question: if learning were content-driven, training on Dora should help most on Dora; instead, the show whose pedagogical loop is more visually anchored (ClubHVQA, 78% object selection) produces a stronger model in either direction. The shared *context-question-pause-answer* structure, not show-specific patterns, is what the model learns.

Generic Training Control. To isolate whether GRPO itself drives the cross-benchmark gains, Table 4(b) trains the same backbones with GRPO on a generic 10K-pair open-ended VQA set (NExT-OE) of matched size. Despite NExT-OE training-set leakage (marked*), SoSVQA scores barely

Table 5: Ablation study. **(a)** Input modality ablation over visual frames (V), transcript (T), and pedagogical context (C). **(b)** Pedagogical structure ablation with all modalities present. A vertical rule separates in-domain benchmarks (DoraVQA, ClubHVQA) from out-of-domain ones (V-MME and NExT-QA). Best results per section in **bold**. †Shared full-model row.

(a) Modality Ablation							(b) Structure Ablation				
V	T	C			V-MME	NExT	Structure			V-MME	NExT
✓	✗	✗	43.42	26.34	60.74	67.91	Random Clips	49.81	41.63	51.70	70.08
✗	✓	✗	50.95	31.88	60.00	70.48	No Pause	45.31	39.43	51.11	72.00
✓	✓	✗	54.72	39.77	61.11	70.83					
✓	✓	✓	**55.11**	**54.45**	**62.20**	**72.86**	Full†	**55.11**	**54.45**	**62.20**	**72.86**

Table 6: Effect of pause-based visual hints on the blue-arrow subset of DoraVQA (frames with arrows ≥ 1, Season 2 excluded). The four conditions vary the spatial signal available at inference: **No hint** (none), **Self-localized** (model's own bbox), **Prompted hint** (textual instruction only), **Oracle box** (ground-truth bbox). *Loc.* reports mean IoU and is only meaningful for *Self-localized*. **Bold**: best overall per column. Underline: best per model.

Model	Condition	Overall	Spatial	Nav.	Know.	Prob. solving	Loc. (mIoU)
Qwen3-VL-8B	No hint	52.24	58.17	35.38	56.10	66.67	–
	Self-localized	53.61	55.83	39.52	64.86	73.61	0.76
	Prompted hint	55.94	64.59	31.54	57.14	79.17	–
	Oracle box	55.25	61.24	45.60	46.15	67.61	–
Qwen3-VL-8B + GRPO	No hint	63.19	70.48	34.62	52.38	86.11	–
	Self-localized	66.98	**80.00**	36.92	**69.05**	83.33	**2.57**
	Prompted hint	**67.61**	77.14	**46.92**	52.38	84.72	–
	Oracle box	**67.61**	77.62	43.85	64.29	**87.50**	–

move from baseline (Qwen3-VL-8B: 56.20/50.75 vs. 55.24/50.67), and transfer to V-MME is also weaker than SoSVQA-joint training (74.44 vs. 80.00). The gap isolates pedagogical structure, not GRPO, as the source of gains.

Context Modalities. Table 5(a) shows the model learns more effectively from transcripts than visual frames (50.95 vs. 43.42 on DoraVQA), consistent with the text-vision asymmetry reported in the Qwen2 technical report [28]. Combining modalities compounds the gain on both shows, with the multimodal jump particularly pronounced on ClubHVQA (V+T: 39.77 vs. T-only: 31.88), reflecting its higher proportion of visually-grounded object-selection tasks.

Pedagogical Structure. Removing the pause segment drops DoraVQA accuracy by 9.80 points, and substituting random (non-pause) clips loses 5.30 points (Table 5(b)). The temporal alignment between question and pause-segment visual evidence is itself a learning signal: the same frames presented without pause alignment recover only part of the gain. To further isolate the two learning signals encoded in the pause—*spatial attention* (where to look) and *entity grounding* (what it is called)—we evaluate four conditions on a held-out blue-arrow subset of DoraVQA, varying how directly the arrow's location is made available to the model (Table 6). Prompting recovers most of the spatial-attention signal but cannot bridge from location to a named entity; only GRPO supervision closes that gap. The pattern holds across model scales up to 72B (Appendix B, Tables 9 and 10), where larger untuned models partially recover spatial attention through scale alone but never match the GRPO-finetuned 8B on entity grounding. Finally, we examine how effectively VLMs leverage the visual cues embedded in pause segments–such as the blue arrows in DoraVQA and the glowing outline in ClubHVQA–that subtly guide viewers toward the correct answer. Full details of this analysis are provided in Appendix B.

5 Conclusion

We demonstrated that the pedagogical structure of children's educational television provides an effective training signal for vision-language reasoning. By fine-tuning Qwen2-VL and Qwen3-VL on just 10K QA pairs from SoSVQA using GRPO, we achieved substantial and generalizable

performance gain on various benchmarks, outperforming models trained on orders of magnitude more data. While our current training relies on only two pedagogical video sources, this work establishes a foundational step toward a comprehensive Pedagogical Interactive Structure (PIS) dataset spanning realistic structured sources (Khan Academy, PhET simulations, classroom recordings) across multiple levels and reasoning domains, all while integrating visual reward modeling to capture motion-based teaching signals during the pause, opening a new chapter for spatial reasoning in VLMs.

References

[1] Sami Abu-El-Haija, Nisarg Kothari, Joonseok Lee, Paul Natsev, George Toderici, Balakrishnan Varadarajan, and Sudheendra Vijayanarasimhan. Youtube-8m: A large-scale video classification benchmark. In *arXiv preprint arXiv:1609.08675*, 2016.

[2] Daniel R Anderson, Jennings Bryant, Alice Wilder, Angela Santomero, Marsha Williams, and Alisha M Crawley. Researching blue's clues: Viewing behavior and impact. *Media Psychology*, 2(2):179–194, 2000. doi: 10.1207/S1532785XMEP0202_4.

[3] Duriye Esra Angın. The effects of Dora the Explorer on preschool children's spatial concept acquisition and spatial ability. *European Scientific Journal*, 13(1):39–53, 2017. doi: 10.19044/esj.2017.v13n1p39.

[4] Shuai Bai, Yuxuan Cai, Ruizhe Chen, Keqin Chen, Xionghui Chen, Zesen Cheng, Lianghao Deng, Wei Ding, Chang Gao, Chunjiang Ge, et al. Qwen3-vl technical report. *arXiv preprint arXiv:2511.21631*, 2025.

[5] Daniel Cores, Michael Dorkenwald, Manuel Mucientes, Cees G. M. Snoek, and Yuki M. Asano. TVBench: Redesigning video-language evaluation. *arXiv preprint arXiv:2410.07752*, 2024.

[6] Google DeepMind. Gemini 3.1 pro model card. `https://deepmind.google/models/model-cards/gemini-3-1-pro/`, February 2026. Published 19 February 2026. Accessed 2026-05-06.

[7] Chaoyou Fu, Yuhan Dai, Yongdong Luo, Lei Li, Shuhuai Ren, Renrui Zhang, Zihan Wang, Chenyu Zhou, Yunhang Shen, Mengdan Zhang, et al. Video-mme: The first-ever comprehensive evaluation benchmark of multi-modal llms in video analysis. In *Proceedings of the Computer Vision and Pattern Recognition Conference*, pages 24108–24118, 2025.

[8] Xingyu Fu, Yushi Hu, Bangzheng Li, Yu Feng, Haoyu Wang, Xudong Lin, Dan Roth, Noah A. Smith, Wei-Chiu Ma, and Ranjay Krishna. Blink: Multimodal large language models can see but not perceive. In *ECCV*, 2024.

[9] Bobs Gannaway. Mickey mouse clubhouse. Television series. Disney Channel (Playhouse Disney/Disney Junior), 2006. Produced by Disney Television Animation. 4 seasons, 125 episodes, 2006–2016.

[10] Daya Guo, Dejian Yang, Haowei Zhang, Junxiao Song, Peiyi Wang, Qihao Zhu, Runxin Xu, Ruoyu Zhang, Shirong Ma, Xiao Bi, et al. Deepseek-r1: Incentivizing reasoning capability in llms via reinforcement learning. *arXiv preprint arXiv:2501.12948*, 2025.

[11] Wenyi Hong, Yean Cheng, Zhuoyi Yang, Weihan Wang, Lefan Wang, Xiaotao Gu, Shiyu Huang, Yuxiao Dong, and Jie Tang. MotionBench: Benchmarking and improving fine-grained video motion understanding for vision language models. In *Proceedings of the IEEE/CVF Conference on Computer Vision and Pattern Recognition (CVPR)*, 2025.

[12] Will Kay, Joao Carreira, Karen Simonyan, Brian Zhang, Chloe Hillier, Sudheendra Vijayanarasimhan, Fabio Viola, Tim Green, Trevor Back, Paul Natsev, et al. The kinetics human action video dataset. *arXiv preprint arXiv:1705.06950*, 2017.

[13] Woosuk Kwon, Zhuohan Li, Siyuan Zhuang, Ying Sheng, Lianmin Zheng, Cody Hao Yu, Joseph E. Gonzalez, Hao Zhang, and Ion Stoica. Efficient memory management for large language model serving with pagedattention. In *Proceedings of the ACM SIGOPS 29th Symposium on Operating Systems Principles*, 2023.

[14] Kunchang Li, Yali Wang, Yinan He, Yizhuo Li, Yi Wang, Yi Liu, Zun Wang, Jilan Xu, Guo Chen, Ping Luo, Limin Wang, and Yu Qiao. MVBench: A comprehensive multi-modal video understanding benchmark. In *Proceedings of the IEEE/CVF Conference on Computer Vision and Pattern Recognition (CVPR)*, pages 22195–22206, 2024.

[15] Bin Lin, Yang Ye, Bin Zhu, Jiaxi Cui, Munan Ning, Peng Jin, and Li Yuan. Video-llava: Learning united visual representation by alignment before projection. In *Proceedings of the 2024 conference on empirical methods in natural language processing*, pages 5971–5984, 2024.

[16] Deborah L Linebarger and Dale Walker. Infants' and toddlers' television viewing and language outcomes. *American Behavioral Scientist*, 48(5):624–645, 2005. doi: 10.1177/0002764204271505.

[17] Antoine Miech, Dimitri Zhukov, Jean-Baptiste Alayrac, Makarand Tapaswi, Ivan Laptev, and Josef Sivic. Howto100m: Learning a text-video embedding by watching hundred million narrated video clips. In *Proceedings of the IEEE/CVF international conference on computer vision*, pages 2630–2640, 2019.

[18] Roni Paiss, Ariel Ephrat, Omer Tov, Shiran Zada, Inbar Mosseri, Michal Irani, and Tali Dekel. Teaching CLIP to count to ten. In *Proceedings of the IEEE/CVF International Conference on Computer Vision (ICCV)*, pages 3170–3180, 2023.

[19] John Schulman, Filip Wolski, Prafulla Dhariwal, Alec Radford, and Oleg Klimov. Proximal policy optimization algorithms. *arXiv preprint arXiv:1707.06347*, 2017.

[20] Ziyao Shangguan, Chuhan Li, Yuxuan Ding, Yanan Zheng, Yilun Zhao, Tesca Fitzgerald, and Arman Cohan. TOMATO: Assessing visual temporal reasoning capabilities in multimodal foundation models. In *International Conference on Learning Representations (ICLR)*, 2025.

[21] Zhihong Shao, Peiyi Wang, Qihao Zhu, Runxin Xu, Junxiao Song, Xiao Bi, Haowei Zhang, Mingchuan Zhang, YK Li, Yang Wu, et al. Deepseekmath: Pushing the limits of mathematical reasoning in open language models. *arXiv preprint arXiv:2402.03300*, 2024.

[22] Haozhan Shen, Peng Liu, Jingcheng Li, Chunxin Fang, Yibo Ma, Jiajia Liao, Qiaoli Shen, Zilun Zhang, Kangjia Zhao, Qianqian Zhang, Ruochen Xu, and Tiancheng Zhao. VLM-R1: A stable and generalizable R1-style large vision-language model. *arXiv preprint arXiv:2504.07615*, 2025.

[23] Aaditya Singh, Adam Fry, Adam Perelman, Adam Tart, Adi Ganesh, Ahmed El-Kishky, Aidan McLaughlin, Aiden Low, AJ Ostrow, Akhila Ananthram, et al. Openai gpt-5 system card. *arXiv preprint arXiv:2601.03267*, 2025.

[24] Yansong Tang, Dajun Ding, Yongming Rao, Yu Zheng, Danyang Zhang, Lili Zhao, Jiwen Lu, and Jie Zhou. Coin: A large-scale dataset for comprehensive instructional video analysis. In *Proceedings of the IEEE/CVF Conference on Computer Vision and Pattern Recognition*, pages 1207–1216, 2019.

[25] Tristan Thrush, Ryan Jiang, Max Bartolo, Amanpreet Singh, Adina Williams, Douwe Kiela, and Candace Ross. Winoground: Probing vision and language models for visio-linguistic compositionality. In *Proceedings of the IEEE/CVF Conference on Computer Vision and Pattern Recognition (CVPR)*, pages 5238–5248, 2022.

[26] Shengbang Tong, Zhuang Liu, Yuexiang Zhai, Yi Ma, Yann LeCun, and Saining Xie. Eyes wide shut? exploring the visual shortcomings of multimodal llms. In *Proceedings of the IEEE/CVF conference on computer vision and pattern recognition*, pages 9568–9578, 2024.

[27] Valerie Walsh Valdes, Chris Gifford, and Eric Weiner. Dora the explorer. Television series, 2000–2019. Nickelodeon Animation Studio.

[28] Peng Wang, Shuai Bai, Sinan Tan, Shijie Wang, Zhihuan Fan, Jinze Bai, Keqin Chen, Xuejing Liu, Jialin Wang, Wenbin Ge, et al. Qwen2-vl: Enhancing vision-language model's perception of the world at any resolution. *arXiv preprint arXiv:2409.12191*, 2024.

[29] Shengao Wang, Arjun Chandra, Aoming Liu, Venkatesh Saligrama, and Boqing Gong. BabyVLM: Data-efficient pretraining of VLMs inspired by infant learning. In *Proceedings of the IEEE/CVF International Conference on Computer Vision (ICCV)*, pages 1380–1390, 2025.

[30] Yi Wang, Kunchang Li, Xinhao Li, Jiashuo Yu, Yinan He, Guo Chen, Baoqi Pei, Rongkun Zheng, Zun Wang, Yansong Shi, et al. Internvideo2: Scaling foundation models for multimodal video understanding. In *European conference on computer vision*, pages 396–416. Springer, 2024.

[31] Zhiqiang Wang, Pengbin Feng, Yanbin Lin, Shuzhang Cai, Zongao Bian, Jinghua Yan, and Xingquan Zhu. CrowdVLM-R1: Expanding R1 ability to vision language model for crowd counting using fuzzy group relative policy reward. *arXiv preprint arXiv:2504.03724*, 2025.

[32] Junbin Xiao, Xindi Shang, Angela Yao, and Tat-Seng Chua. Next-qa: Next phase of question-answering to explaining temporal actions. In *Proceedings of the IEEE/CVF conference on computer vision and pattern recognition*, pages 9777–9786, 2021.

[33] Dejing Xu, Zhou Zhao, Jun Xiao, Fei Wu, Hanwang Zhang, Xiangnan He, and Yueting Zhuang. Video question answering via gradually refined attention over appearance and motion. In *ACM Multimedia*, 2017.

[34] Kaichen Zhang, Bo Li, Peiyuan Zhang, Fanyi Pu, Joshua Adrian Cahyono, Kairui Hu, Shuai Liu, Yuanhan Zhang, Jingkang Yang, Chunyuan Li, et al. Lmms-eval: Reality check on the evaluation of large multimodal models. In *Findings of the Association for Computational Linguistics: NAACL 2025*, pages 881–916, 2025.

[35] Yuanhan Zhang, Jinming Wu, Wei Li, Bo Li, Zejun Ma, Ziwei Liu, and Chunyuan Li. Llava-video: Video instruction tuning with synthetic data. *arXiv preprint arXiv:2410.02713*, 2024.

[36] Dimitri Zhukov, Jean-Baptiste Alayrac, Ramazan Gokberk Cinbis, David Fouhey, Ivan Laptev, and Josef Sivic. Cross-task weakly supervised learning from instructional videos. In *Proceedings of the IEEE/CVF Conference on Computer Vision and Pattern Recognition*, pages 3537–3545, 2019.

A Hyperparameter Sweeps

We conduct sequential hyperparameter sweeps to identify optimal GRPO training configurations. Each sweep fixes previously optimized hyperparameters while varying a single dimension.

Table 7: Sequential hyperparameter sweeps for GRPO training. Each sweep fixes previously optimized parameters. Bold indicates selected values used in main experiments.

Parameter	Values Tested	Selected	DoraVQA
KL Coefficient	{0.0, 0.001, **0.01**, 0.1}	**0.01**	{42.96, 40.71, **46.38**, 45.19}
Learning Rate	{1e-6, 1e-5, **1e-4**, 1e-3}	**1e-4**	{43.69, 45.19, **50.09**, 38.89}
Reward Scaling	{0.5, 1.0, **2.0**, 5.0}	**2.0**	{45.92, 45.19, **45.69**, 43.93}

Table 7 presents our hyperparameter optimization results. The KL coefficient controls the divergence penalty between the policy and reference model; we find 0.01 provides the best balance, with both higher (0.1) and lower (0.001) values degrading performance. For learning rate, 1e-4 achieves optimal performance (50.09%), while higher rates (1e-3) cause training instability (38.89%) and lower rates (1e-6) result in insufficient learning. Reward scaling at 2.0 provides marginal improvements over the default 1.0, amplifying the learning signal from correct answers without overwhelming the policy gradient.

Table 8 examines training duration and overfitting characteristics. Qwen2-VL-7B peaks at 150 steps (62.96%) before degrading sharply at 250 steps (56.0%), indicating overfitting to the narrow educational domain. Qwen3-VL-2B shows more robust training, peaking later at 250 steps (67.97%) with gradual performance decline. These results highlight the importance of early stopping when fine-tuning on domain-specific content to preserve generalization capabilities.

Table 8: Ablation study on training steps for both models. Performance peaks at between 150 and 250 steps then degrades due to overfitting on the narrow educational domain.

Model	50	100	150	200	250	300
Qwen2-VL-7B	57.49	60.29	**62.96**	60.98	56.00	60.84
Qwen3-VL-2B	63.67	66.67	65.91	65.54	**67.97**	66.60

Based on these sequential sweeps, we use KL coefficient = 0.01, learning rate = 1e-4, and reward scaling = 2.0 for all main experiments reported in this paper. Training duration is set at 150 steps for Qwen2-VL-7B and 250 steps for Qwen3-VL-2B to avoid overfitting while maximizing in-domain performance.

B Pause Visual Hint Analysis

A central hypothesis of this work is that the *pause* segment in the *context–question–pause–answer* structure functions as an implicit reasoning trace: it visually isolates the evidence required to answer the question, thereby grounding language in perception. To test whether this signal is recoverable by an off-the-shelf vision-language model, we design a controlled prompting experiment that makes the show's blue-arrow hint explicitly available to the model, and measure how much of the resulting gain requires GRPO fine-tuning versus prompt engineering alone. To enable this analysis and support future spatial-grounding work, we manually annotated 702 bounding boxes around the blue directional arrows that appear during *Dora the Explorer* pause segments, released alongside the SoSVQA pipeline.

Setup. We evaluate four conditions on a held-out subset of DoraVQA examples that contain a visible blue directional arrow during the pause segment. The conditions form an intervention-strength ladder over the spatial signal available at inference:

- **No hint.** Standard inference; the model is not told the arrow exists.

- **Self-localized.** The model emits a bounding box for the arrow in a first pass and conditions on its own (noisy) prediction in a second pass.

- **Prompted hint.** The model receives a textual instruction: *"Locate the blue arrow in the image. Use its bounding-box coordinates to identify the object or region it is pointing at, and use that information to answer the question."*—no coordinates are produced or supplied externally.

- **Oracle box.** The ground-truth bounding box of the arrow is supplied directly in the prompt.

We additionally evaluate each condition with our **+ GRPO** fine-tuned model. All conditions use identical visual frames and question text; the only variables are the system prompt and whether the model weights have been fine-tuned.

Qualitative findings. Figure 4 illustrates two representative examples. In *Example 1* ("Who is the strongest one in the team?"), the baseline hallucinates an incorrect character. The oracle box redirects visual attention to the correct spatial region, but the model describes the referent only at the level of a perceptual property ("the blue animal"), failing to resolve the arrow to a named entity. Only GRPO fine-tuning enables the full inference chain—from arrow location, to object identity, to the correct named answer (Benny the bull). In *Example 2* ("What makes you sneeze?"), the hint alone is sufficient: the arrow unambiguously isolates a single salient object (the pepper shaker), requiring no entity-level knowledge to name correctly. Both oracle conditions succeed here, while the no-hint condition fails entirely.

Interpretation. These examples reveal a consistent two-stage failure mode in models without GRPO. First, without the hint, the model does not attend to the pause arrow at all, defaulting to plausible but incorrect priors from its pre-training distribution. Second, even when the hint redirects attention, the model can localize a region without being able to resolve it to a named entity—a gap that GRPO training on pedagogically structured content bridges by repeatedly supervising the full reasoning chain from visual evidence to grounded answer. This suggests that the pause arrow encodes two distinct learning signals: a *spatial attention* signal (where to look) that is recoverable through prompting, and an *entity grounding* signal (what it is called) that requires the kind of structured supervision our dataset provides. The quantitative results for this ablation are reported in Table 6.

Scaling behavior. To test whether scale alone recovers the pause signal, we evaluate the same conditions on larger untuned models (Table 9). Qwen2.5-VL-72B with prompted hint (60.66%) trails the GRPO-finetuned 8B model (67.61%), confirming that scale partially recovers spatial attention but does not replace structured supervision for entity grounding. Qwen2.5-VL-72B does achieve 11.87% mean IoU for arrow localization vs. $<3\%$ for the 8B models, indicating that spatial localization benefits more directly from scale than entity resolution does.

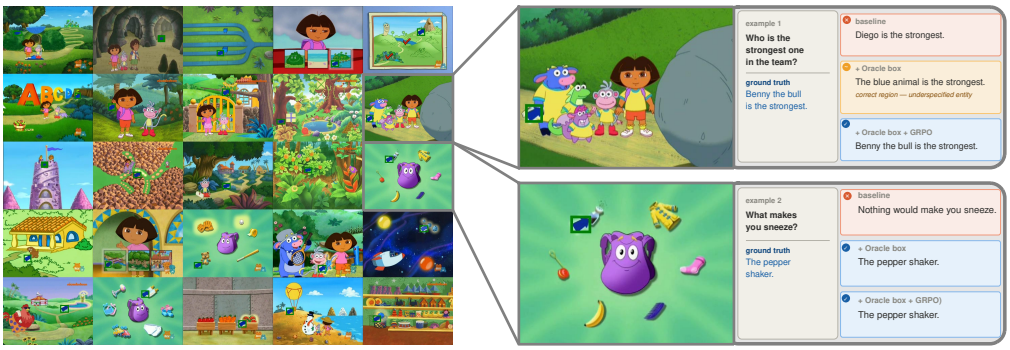


Figure 4: **Effect of pause-based visual hints on spatial grounding.** We evaluate three conditions on two examples drawn from *Dora the Explorer*'s pedagogical pause segments, where a blue arrow highlights the visually salient object relevant to the question. **(No hint)** receives only the raw frame and question with no additional guidance. **(+ Oracle box)** additionally supplies the ground-truth bounding box of the arrow's target region as part of the prompt. **(+ Oracle box + GRPO)** combines the same oracle box with our GRPO-finetuned model. In *Example 1*, the baseline hallucinates an incorrect character (Diego); the oracle box redirects attention to the correct spatial region but the untuned model describes the referent only at the level of a perceptual property ("the blue animal"), failing to resolve it to a named entity. Only GRPO fine-tuning enables the model to bridge from spatial location to the correct named answer (Benny the bull). In *Example 2*, both conditions succeed, confirming that an unambiguous spatial hint is sufficient for object-level queries that require no entity-level knowledge. Together, these results demonstrate that the show's pause arrow functions as an *implicit reasoning trace*: it constrains the visual search space, but generalizing from spatial localization to grounded entity recognition requires the structured supervision provided by GRPO training on pedagogical content.

Table 9: Pause-based visual hint results across model scales (blue-arrow subset). Same setup and conditions as Table 6. Qwen3-VL-8B + GRPO (8B) surpasses both Qwen3-VL-30B and Qwen2-VL-72B on overall accuracy, while Qwen2.5-VL-72B is the only untuned model with meaningful localization (11.87% mIoU). The *self-localized* condition degrades Qwen3-VL-30B sharply (35.19 vs. 55.52 overall), revealing that the coordinate-emission pathway is unstable at this scale—whereas the *prompted hint*, which carries no coordinates, is robust across all model sizes. **Bold**: best overall per column. Underline: best per model.

Model	Condition	Overall	Spatial	Nav.	Know.	Loc. (mIoU)
Qwen3-VL-8B	No hint	52.24	58.17	35.38	56.10	–
	Self-localized	53.61	55.83	39.52	64.86	0.76
	Prompted hint	55.94	64.59	31.54	57.14	–
	Oracle box	55.25	61.24	45.60	46.15	–
Qwen3-VL-8B + GRPO	No hint	63.19	70.48	34.62	52.38	–
	Self-localized	66.98	**80.00**	36.92	**69.05**	2.57
	Prompted hint	**67.61**	77.14	**46.92**	52.38	–
	Oracle box	**67.61**	77.62	43.85	64.29	–
Qwen3-VL-30B	No hint	55.52	63.24	25.81	48.78	–
	Self-localized	35.19	39.80	19.49	39.47	0.00
	Prompted hint	54.37	63.05	28.00	51.28	–
	Oracle box	52.69	59.90	30.17	61.11	–
Qwen2-VL-72B	No hint	52.85	57.62	31.78	52.38	–
	Self-localized	56.24	63.81	36.15	50.00	2.03
	Prompted hint	55.45	64.29	33.85	64.29	–
	Oracle box	55.45	61.90	33.85	59.52	–
Qwen2.5-VL-72B	No hint	56.56	61.90	40.00	50.00	–
	Self-localized	54.19	56.19	34.62	61.90	**11.87**
	Prompted hint	60.66	66.19	40.77	59.52	–
	Oracle box	58.77	65.71	42.31	64.29	–

Table 10: Arrow localization accuracy across model scales (*self-localized* condition only, where coordinates are externalized). IoU@k reports the percentage of predictions exceeding the given threshold. The GRPO-finetuned 8B model (2.57% mIoU) outperforms both the 30B and 72B untuned models, demonstrating that structured supervision recovers spatial localization more effectively than scaling alone.

Model	IoU@10	IoU@25	IoU@50	IoU@75	mIoU
Qwen3-VL-8B	0.00	0.00	<1	<1	0.76
Qwen3-VL-8B + GRPO	0.00	0.00	<1	<1	2.57
Qwen3-VL-30B	0.00	0.00	0.00	0.00	0.00
Qwen2-VL-72B	6.96	0.63	0.00	0.00	2.03
Qwen2.5-VL-72B	**35.51**	**20.22**	**5.10**	**0.80**	**11.87**

C Additional Qualitative Results

Figure 5 presents two challenging examples from SoSVQA that illustrate distinct failure modes of baseline models. The spatial location example (left) demonstrates partial occlusion: Swiper the fox is only partially visible behind Dora, requiring the model to recognize an object from incomplete visual information. Without GRPO fine-tuning, Qwen2-VL-2B fails to detect the occluded character entirely, while the GRPO-finetuned variant correctly identifies his location consistent with the spatial perception gains reported in Table 1. The deixis resolution example (right) illustrates a subtler failure mode. The question "Mickey, what's that?" cannot be resolved by identifying the most visually salient object in the frame; it requires grounding the referent *what* in the episode's narrative context. Baseline models default to describing visually dominant elements (the colorful bus) or arbitrarily salient objects (a tree stump), answering "what is visually prominent?" rather than "what is Mickey referring to?". Our GRPO-finetuned models correctly resolve the reference to the drum by grounding the question in the episodic context; the same entity grounding signal that the *context-question-pause-answer* structure supervises directly (Section B). Together, these examples demonstrate that GRPO fine-tuning on pedagogically structured content improves both spatial perception under occlusion and narrative-grounded reference resolution. **Additional interactive qualitative results.** We provide an interactive HTML page in the supplementary materials with further visual examples across all task types. Please open `supplementary/index.html` in a web browser to explore the full set of qualitative results beyond the examples shown in this paper.

D Prompt Templates

To support full reproducibility, this section documents the exact message structures used during GRPO training and multiple-choice evaluation. Visual frames are uniformly sampled from the video segment associated with each question; placeholders of the form <...> are filled in per-example at runtime.

D.1 Frame Sampling

For every training and evaluation example, we uniformly sample N frames from the video segment $[t_{\text{start}}, t_{\text{end}}]$ associated with the question, where t_{start} is the beginning of the *context* segment and t_{end} is the end of the *pause* segment. Sampled frames are denoted <*frame_1*>, ..., <*frame_n*>, and are passed in temporal order. We use N=4 unless otherwise noted; the prompt structure is independent of N.

D.2 GRPO Training Prompt

During GRPO training, the model receives the sampled frames together with the episode transcript (with <*pause*> tokens inserted at scene boundaries to mark the pedagogical pause), the question, and an open-ended `Answer:` cue. Free-form generations are scored against the ground-truth answer a^* using the reward defined in Eq. 1.

GRPO Training Message (Open-Ended Generation)

```
messages = [
    {
        "role": "user",
        "content": [
            {"type": "image", "image": <frame_1>},
            {"type": "image", "image": <frame_2>},
            # ... uniformly sampled frames in temporal order ...
            {"type": "image", "image": <frame_n>},
            {
                "type": "text",
                "text": (
                    "You are a helpful visual reasoning assistant for kids.\n"
                    "Think step by step, then give a final concise answer.\n"
                    "Context: <transcript_with_pause_tokens>\n"
                    "Question: <question_text>\n"
                    "Answer:"
                ),
            },
        ],
    },
]
```

D.3 Multiple-Choice Evaluation Prompt

All cross-benchmark evaluations (Video-MME, NExT-QA, MVBench, MotionBench, TVBench) and the in-domain SoSVQA evaluation use the multiple-choice format below. The model is constrained to emit a single digit selecting one of four choices, which we parse directly. As noted in Section 3.2, this deliberate format mismatch with training isolates transferable reasoning from answer-format memorization.

Multiple-Choice Evaluation Message (Single-Digit Output)

```
messages = [
    {
        "role": "user",
        "content": [
            {"type": "image", "image": <frame_1>},
            {"type": "image", "image": <frame_2>},
            # ... uniformly sampled frames in temporal order ...
            {"type": "image", "image": <frame_n>},
            {
                "type": "text",
                "text": (
                    "You are a helpful visual reasoning assistant for kids.\n"
                    "Think step by step and choose one correct choice "
                    "from 0, 1, 2 or 3.\n"
                    "Only return one single digit as the best answer.\n"
                    "Context: <transcript_with_pause_tokens>\n"
                    "Question: <question_text>\n"
                    "Choices: {\"0\": \"choice_A\", \"1\": \"choice_B\", "
                    "\"2\": \"choice_C\", \"3\": \"choice_D\"}"
                ),
            },
        ],
    },
]
```

Component	Training (GRPO)	Evaluation (MCQ)
Frames	N uniformly sampled, temporal order	N uniformly sampled, temporal order
Context	Transcript with <*pause*> tokens	Transcript with <*pause*> tokens
Question	Free-form question text	Free-form question text
Choices	✗ (none)	✓ JSON dict, keys 0–3
Output target	Open-ended answer string	Single digit $\in \{0, 1, 2, 3\}$
Scoring	Reward (Eq. 1) vs. a^*	Exact-match top-1 accuracy

Table 11: Differences between training and evaluation prompts. The training prompt is open-ended; the evaluation prompt adds explicit multiple-choice formatting and constrains the output to a single digit.

D.4 Summary of Prompt Components

E Data Access and Licensing

SoSVQA does not redistribute any video frames, audio, or raw episode files. All visual and audio content was collected from publicly available YouTube uploads and remains hosted by the original rights holders. Users are required to independently obtain access to the corresponding episodes under YouTube's existing terms of service. We release episode identifiers, temporal timestamps, question-answer annotations, choices, transcript span indices, manually annotated bounding box for the pause-segment visual cues along with the code to align these annotations. As the source material consists of publicly broadcast children's educational programming, the datasets do not introduce new privacy risks; nevertheless, SoSVQA is intended strictly for research and evaluation purposes, and we discourage any use outside this scope.

F MCQ Generation and Manual Auditing

To convert the open-ended QA pairs extracted from the *context-question-pause-answer* structure into a multiple-choice evaluation format, we use Google Gemini 2.5 Flash to (i) simplify the gold answer into a concise, MCQ-appropriate phrase and (ii) generate three plausible but incorrect distractors of similar style and length. The text-only prompt operates on the question, gold answer, and surrounding transcript context (truncated to the most recent 1,000 characters when longer), and returns a structured JSON object with the simplified answer and distractors. The exact prompt template is shown below.

Gemini MCQ Generation Prompt (Text-Only)

```
Create a multiple-choice question with <num_distractors> wrong answer options.

VIDEO CONTEXT:
<transcript_context>

QUESTION: <question_text>
ORIGINAL CORRECT ANSWER: <gold_answer>

TASK:
1. First, simplify the original correct answer to be concise and
   MCQ-appropriate (similar length to distractors, clear and direct)
2. Then generate <num_distractors> wrong but plausible answers that match
   the answer style and length

REQUIREMENTS:
- Simplified answer: Short, clear, direct (1-2 sentences max,
  ideally 1 phrase)
- Distractors: Each must be incorrect, believable, simple words for
  ages 3-7, unique, and similar length to the simplified answer

OUTPUT FORMAT - Copy this structure exactly and fill in all fields:
```

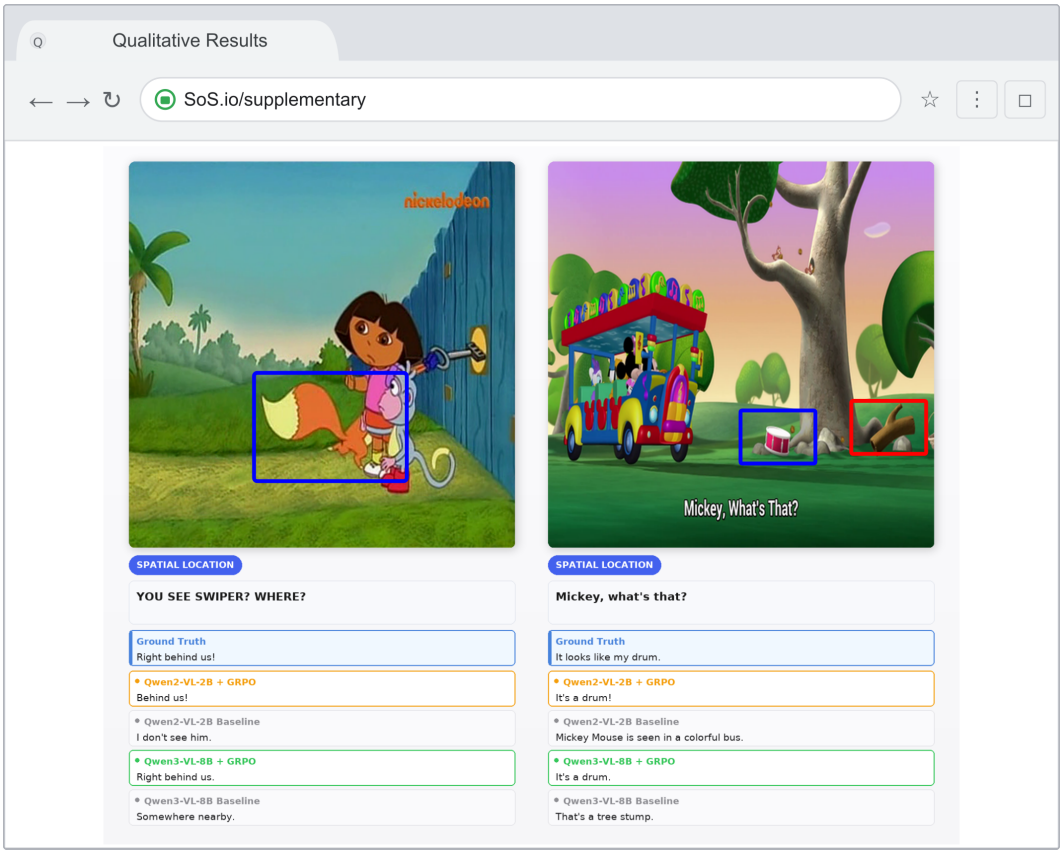


Figure 5: **Additional challenging examples from SoSVQA.** Left: Spatial location task where Swiper the fox is partially occluded behind a blue wall, requiring the model to recognize objects from incomplete visual information (blue box). Right: A deixis resolution task where the question "Mickey, what's that?" requires understanding *what* Mickey is referring to within the episodic narrative context. Baseline models either describe the dominant visual element (the colorful bus) or latch onto an unrelated object—the tree stump (red box)—revealing that they answer "what is visually prominent?" rather than "what is Mickey referring to?". Our GRPO-finetuned models correctly resolve the reference to the drum (blue box) by grounding the question in the episode's narrative context. **Additional interactive qualitative results.** We provide an interactive HTML page in the supplementary materials with further visual examples across all task types. Please open `supplementary/index.html` in a web browser to explore the full set of qualitative results beyond the examples shown in this paper.

```
{
    "simplified_answer": "concise version of the correct answer",
    "distractor_1": "your first wrong answer",
    "distractor_2": "your second wrong answer",
    "distractor_3": "your third wrong answer"
}

IMPORTANT:
- Simplify the answer to be concise (like the distractors will be)
- You must provide simplified_answer, distractor_1, distractor_2, AND
  distractor_3. All fields are required.
```

Generation uses temperature 0.5, top-$p = 0.95$, and a maximum of $2{,}048$ output tokens. Each candidate MCQ is post-processed to enforce case-insensitive uniqueness between the simplified answer and distractors, and to discard any item that does not yield at least three unique distractors after deduplication.

Manual auditing of deictic answers. Although Gemini reliably produces fluent distractors, a recurring failure mode arises from the pedagogical structure itself: many answers in the source material are *deictic*—phrases such as "there it is," "here it is," or "right there" that derive their meaning from the on-screen visual hint (e.g., a directional arrow or character gesture) rather than from any named entity. When such a phrase becomes the gold MCQ option alongside three named-entity distractors generated from the transcript, the resulting item is trivially solvable by surface form alone: the deictic phrase is the only choice that does not name a specific entity, leaking the correct answer without requiring any visual reasoning.

To eliminate this shortcut, we manually audited every MCQ whose simplified answer or original answer contained a deictic marker (*there it is*, *here it is*, *right there*, and minor morphological variants). The audit identified **106 affected items in DoraVQA and 31 in ClubHVQA**. For each affected item, we manually rewrote the four choices so that all options share a consistent surface form—typically a yes/no acknowledgement paired with a directional or perceptual claim—forcing the model to ground the answer in the visual scene rather than in lexical type. Figure 6 shows a representative before/after example.

Concretely, the question *"Now, where's the quiet forest? Do you see the quiet forest?"* originally paired the deictic gold answer *"There it is!"* against three named-location distractors (*Little bird?*, *Yellow Valley?*, *Big mountain?*), so the answer could be selected purely by recognizing which option is not a named location. After auditing, the four choices become parallel yes/no–directional statements (*Yes, it's on the left.*, *No, I can't see it.*, *Yes, it's on the right.*, *I see flowers.*), which can only be resolved by attending to the on-screen arrow during the pause segment.

This audit affects $106/5{,}348 = 1.98\%$ of DoraVQA and $31/4{,}652 = 0.67\%$ of ClubHVQA. The lower rate in ClubHVQA is consistent with its more visually-driven, object-selection-dominated structure (78% object selection; Figure 1), in which gold answers are typically named objects rather than deictic references. All audited items are released as part of the SoSVQA annotations, with both the original and revised choice sets preserved for transparency.

G Limitations

While SoSVQA demonstrates that pedagogical structure enables stronger spatial reasoning abilities for VLMs despite limited data scale, the approach has several limitations. First, the dataset depends on the availability and quality of publicly hosted videos and corresponding transcripts; oftentimes the alignment between SRT files and episode timestamps is imperfect and requires human input. Misaligned or noisy subtitles can introduce extraction errors, especially in fast-paced scenes or episodes with inconsistent caption timing. Second, SoSVQA currently draws from only two children's educational programs–Dora the Explorer and Mickey Mouse Clubhouse. Although these shows share a strong context-question-pause-answer structure, they represent a narrow slice of pedagogical video, and broader generalization would require incorporating additional sources with diverse reasoning styles and visual environments. Third, despite improvements from GRPO fine-tuning, counting performance remains a persistent challenge: models still struggle with fine-grained enumeration,

Question: *Now, where's the quiet forest? Do you see the quiet forest?*
Gold answer: *Yes– there it is* $\rightarrow$ *There it is!*



Pause segment: Boots is pointing to the quiet forest on the right.

Before audit : shortcut leak

- Little bird?
- Yellow Valley?
- **There it is! ✓**
- Big mountain?

The deictic gold answer is the only non-entity option—selectable by surface form alone.

After audit : visually grounded

- Yes, it's on the left.
- No, I can't see it.
- **Yes, it's on the right. ✓**
- I see flowers.

All four options share a parallel yes/no–directional surface form, requiring the model to ground the answer in the on-screen arrow.

Figure 6: Manual audit of deictic gold answers in SoSVQA. The original choice set leaks the answer through surface form; "There it is!" is the only non-named-entity option and can be selected without attending to the visual scene. The audited choice set forces visual grounding by making all four options parallel directional statements. We applied this audit to all 106 deictic items in DoraVQA and 31 in ClubHVQA.

and the gains observed in counting tasks are modest relative to other reasoning categories. Fourth, due to limited hardware availability, we evaluate only a small set of open-source VLM families and parameter scales. Larger models and alternative architectures may benefit more from structured supervision, but we were unable to explore these directions. Together, these limitations highlight opportunities for expanding the dataset, improving alignment quality, and scaling evaluations to a wider range of model families and pedagogical sources.

H Compute Resource

For the Qwen2-7B and Qwen3-8B models, all GRPO fine-tuning runs were trained for 450 epochs on a single NVIDIA H200 GPU with an 8-core CPU and 64 GB of system memory. Each model used a combined batch size of 8, gradient accumulation of 4, and 8 sampled generations per prompt. Optimization followed standard GRPO settings, with a learning rate of 1e-4, KL-regularization coefficient β=0.01, and reward weight of 2.0, informed by our parameter sweep results. For the 2B variants, training was performed on a single NVIDIA A100 GPU, while all other hyperparameters and training configurations remained unchanged. Each individual fine-tuning run required approximately 7-8 GPU hours on the H200 or A100, depending on the model size and checkpoint-resume behavior. Across all models, ablations, and joint-training configurations, the total compute used for the experiments reported in the paper amounts to roughly 120-150 GPU-hours. The full research project required additional compute beyond the final reported experiments, including preliminary GRPO reward weight sweeps, early alignment-quality diagnostics, and several failed or discarded runs; these exploratory stages added an estimated 40-60 GPU-hours.

Inference was conducted using the default settings provided by LMMS-Eval [34] and VLLM [13], running across a heterogeneous pool of GPUs–including NVIDIA V100, A100, A5000, A6000, H200, and L40S–selected based on model size and input sequence length. Storage requirements were modest: each run required approximately 50-80 GB of temporary workspace for checkpoints, logs, and intermediate outputs. All experiments were conducted on an private high-performance computing (HPC) cluster equipped with GPU nodes accessible through a shared scheduling system.

I Safeguards

In our work, we take several safeguards to ensure responsible use and to minimize risks of misuse or unintended deployment. First, we do not redistribute any copyrighted video frames, audio, or raw episode content. All visual and audio material remains hosted by the original rights holders on YouTube, and users must independently obtain access under YouTube's existing terms of service. We release only episode identifiers, timestamps, transcript spans, question–answer annotations, and manually annotated bounding boxes, which pose minimal risk and contain no personally identifiable information. Second, because the source material consists of publicly broadcast children's educational programming, the dataset does not introduce new privacy risks; nonetheless, we explicitly state that SoSVQA is intended strictly for research and evaluation, and we discourage any use outside this scope.

To further reduce misuse risk, we will provide clear documentation describing the dataset's structure, intended purpose, and limitations, and we avoid releasing any large-scale pre-trained or instruction-tuned models that could be repurposed for harmful applications. Our fine-tuned models are trained only on pedagogically structured QA pairs and do not include any safety-critical capabilities. Finally, we will include usage guidelines in the repository emphasizing that the dataset should not be used for commercial deployment, content generation, or applications involving children, and we provide scripts that require users to supply their own video access, preventing accidental redistribution of copyrighted or sensitive material.

Together, these safeguards ensure that the released assets are responsibly scoped, legally compliant, and suitable for research use without enabling high-risk downstream applications.